Residence time of symmetric random walkers in a strip with large reflective obstacles

Alessandro Ciallella,[1,*] Emilio N. M. Cirillo,[1,†] and Julien Sohier[2,‡]

[1]*Dipartimento di Scienze di Base e Applicate per l'Ingegneria, Sapienza Università di Roma, via A. Scarpa 16, I–00161, Roma, Italy*

[2]*Laboratoire d'Analyse et de Mathématiques Appliquées (LAMA), UMR 8050, Université Paris Est Créteil, 61, avenue du Général de Gaulle, 94010 Créteil Cedex, Paris, France*

(Received 28 November 2017; revised manuscript received 2 February 2018; published 14 May 2018)

We study the effect of a large obstacle on the so-called residence time, i.e., the time that a particle performing a symmetric random walk in a rectangular (two-dimensional, 2D) domain needs to cross the strip. We observe complex behavior: We find out that the residence time does not depend monotonically on the geometric properties of the obstacle, such as its width, length, and position. In some cases, due to the presence of the obstacle, the mean residence time is shorter with respect to the one measured for the obstacle-free strip. We explain the residence time behavior by developing a one-dimensional (1D) analog of the 2D model where the role of the obstacle is played by two defect sites having smaller probability to be crossed with respect to all the other regular sites. The 1D and 2D models behave similarly, but in the 1D case we are able to compute exactly the residence time, finding a perfect match with the Monte Carlo simulations.

DOI: 10.1103/PhysRevE.97.052116

I. INTRODUCTION

When a particle flow crosses a region in the presence of obstacles, different effects can be observed [1,2]. The barriers, depending on the system which is considered, can either speed up or slow down the dynamics.

For example, it is well known that the presence of obstacles can induce a sublinear behavior with respect to time of the mean square distance traveled by particles undergoing Brownian motion. This phenomenon, called *anomalous diffusion*, is observed in cells and in some cases it is explained as an effect due to the presence of macromolecules playing the role of obstacles for diffusing smaller molecules [3–6].

In many other different contexts, it has been proven that the presence of an obstacle can surprisingly accelerate the dynamics. In a granular system, the outgoing flow, dramatically reduced by the clogging at the exit, can be improved by placing an obstacle above the exit [7–10].

A similar phenomenon is observed in pedestrian flows [11–15] in cases of fast egress, where clogging at the door can be reduced by means of suitably positioned obstacles [16–19] that slow down pedestrian accumulation at the door (the possibility of clustering far from the exit due to individual cooperation has been the object of study in Refs. [15,20,21]). These unexpected phenomena are a sort of inverse Braess paradox [22,23]: Adding a road link to a road network can cause cars to take longer to cross the network; here, adding barriers results in a decrease of the time that particles need to cross a region of the space.

These phenomena are discussed here in the very basic scenario of a symmetric random walk and we study the effect of the barriers on the typical time, i.e., the *residence time*, that a particle needs to cross a strip.

In these terms, the residence time issue has been posed in Refs. [24,25], where the flow of particles entering an horizontal strip through the left end, undergoing a random walk with exclusion inside the strip, and exiting it through the right end has been considered [26]. In those papers, a thorough study of the residence time properties as a function of the details of the dynamics, such as the horizontal drift, has been provided and in Ref. [25] two different analytic tools have been developed. In Ref. [24], it has been shown that in some regimes the residence time is not monotonic with respect to the size of the obstacle. This complex behavior has been related to the way in which particles are distributed along the strip at stationarity; more precisely, it has been explained in terms of the occupation number profile, which strongly depends on how particles interact due to the presence of the exclusion rule.

Here, we consider the same geometry, but we assume that particles perform independent random walks in the strip. In other words, we consider the average behavior of a single walker. Nevertheless, we observe surprising features of the system. We find that the residence time is nonmonotonic with respect to the side lengths of the obstacle and the horizontal coordinate of its center. For suitable choices of the obstacle, the residence time in the presence of the barrier is shorter than the one measured for the empty strip. We can say that placing a suitable obstacle in the strip allows us to select those particles that cross the strip in a shorter time. We also find that the same obstacle, placed in different positions along the strip, can either increase or decrease the residence time with respect to the empty strip case. This complex behavior is not intuitive at all; indeed, it would be rather natural to infer that the presence of the obstacle increases the residence time since the channels flanking the obstacles are more difficult to be accessed by the particle.

This problem has been studied in Ref. [27] in the framework of kinetic theory, more precisely for a model with particles

*alessandro.ciallella@uniroma1.it
†emilio.cirillo@uniroma1.it
‡julien.sohier@u-pec.fr

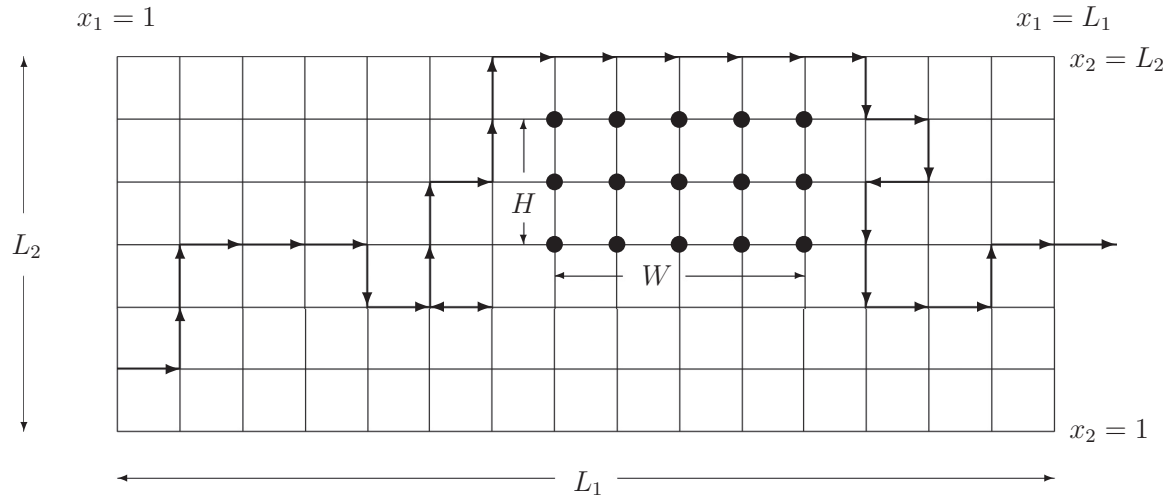

FIG. 1. Representation of the lattice Λ. The circles denote the obstacle made of sites which cannot be accessed by the particle. The parameters H and W are, respectively, the height and the width of the obstacle. Bold arrows denote a trajectory of the 2D random walk entering the lattice from the left and exiting it from the right.

moving according to the linear Boltzmann dynamics. In that paper, a particle moves along a line with constant velocity for a time which is an exponential random variable, and then the particle changes the direction of its motion, simulating the hit with a circular scatterer. We refer the reader to Ref. [27, Section 3] for more details. We stress that the model considered here is totally different from the one in Ref. [27]; nevertheless, if the linear Boltzmann dynamics is observed on a larger space scale, we guess that its behavior must be pretty similar to that of a two-dimensional (2D) random walk. This conjecture is confirmed by the results discussed in Sec. II that are qualitatively similar to those found in Ref. [27]. In particular, also in that case, it has been observed that the residence time is in some cases nonmonotonic with respect to the geometrical parameters of the obstacle, such as its width and position.

We can explain these phenomena as the consequence of the competition between two opposite effects. The time that particles spend in the channels flanking the obstacle is smaller than the total time spent in the central part (the region containing the obstacle) of the strip in the empty case. On the other hand, the time spent by the particles in the regions of the strip on the left and right of the obstacle is larger with respect to the empty case. These effects are due to the fact that it is more difficult for the walker to enter the central region of the strip, namely, one of the two channels formed by the obstacle. The residence time behavior hence depends on which of the two effects dominates the dynamics.

In this paper, we also introduce a one-dimensional (1D) model which mimics the 2D system. The presence of the obstacle is modeled via two defect sites, the left and the right ones. The behavior of the particle sitting on one of these two special sites is similar to the one of the 2D particle moving in the columns adjacent to the obstacle. Indeed, we assume that the probability for the particle sitting on the left (right) defect site to move to its right (left) is smaller than $1/2$. The 1D model is studied both numerically and analytically; i.e., the residence time is computed exactly, even if we could not provide an explicit expression. The match between the numerical data and the analytic solution is perfect. The 1D model shows the same features as the 2D one and also the interpretation of the results is analogous.

The paper is organized as follows. In Sec. II, we introduce the 2D model and discuss the related Monte Carlo results. In Sec. III, we propose the 1D analog and discuss both the numerical and the exact results. In Sec. IV, we prove the exact results. Finally, in Sec. V, we summarize our conclusions.

II. THE 2D MODEL

A particle performs a symmetric simple random walk on the 2D strip $\Lambda = \mathbb{Z}^2 \cap [0,L_1] \times [0,L_2] \subset \mathbb{Z}^2$; see Fig. 1, where L_1 and L_2 are two positive integer numbers. Equivalently,

$$\Lambda = \{x = (x_1,x_2), x_1 \in \{1,\dots,L_1\}, x_2 \in \{1,\dots,L_2\}\},$$

where we mean that the two integer variables x_i, with $i = 1,2$, vary in the sets $\{1,2,3,\dots,L_i\} \subset \mathbb{Z}$; namely, x_i is a generic integer number larger or equal to 1 and smaller or equal to L_i. A similar notation is often used in the sequel.

The 1 and 2 directions are respectively called *horizontal* and *vertical*. The particle starts at a site in the first column on the left, namely, at a site $(1,x_2)$ with $x_2 = 1,\dots,L_2$ chosen at random with uniform probability. At each unit of time, the particle performs a move to one of the four neighboring sites with the same probability $1/4$. If the target site is in the horizontal boundary, that is, it belongs to the set $\{(x_1,0), x_1 \in \{1,\dots,L_1\}\} \cup \{(x_1,L_2+1), x_1 \in \{1,\dots,L_1\}\}$, the particle does not move, which means that the horizontal boundary is a reflecting surface. If the target site belongs to the left or to the right vertical boundary $\{(0,x_2), x_2 \in \{1,\dots,L_2\}\} \cup \{(L_1+1,x_2), x_2 \in \{1,\dots,L_2\}\}$, the particle exits the system and the walk is stopped. Moreover, we shall consider a rectangular obstacle inside the strip, in the sense that, when one of the sites of this region will be chosen as target site for the move of the particle, the particle will not move. Thus, the sites in the obstacle are not accessible to the

walker. The width and the height of the obstacle will be denoted respectively by W and H.

The *residence time* is defined as the mean time that the particle which started at a uniformly chosen random site with abscissa $x_1 = 1$ takes to exit the strip through the right boundary. Sometimes, we shall address to the residence time as to the *total* residence time to stress that it refers to the total time that the particle spends inside the strip. More precisely, one could consider the walk on the infinite strip $\mathbb{Z} \times \{1, \ldots, L_2\}$ and define the residence time as the mean of the first hitting time for a particle started at a site $(1,x_2)$, with $x_2 = 1, \ldots, L_2$ chosen at random with uniform probability, to the set of sites with $x_1 = L_1 + 1$ conditioned to the event that the particle reaches such a subset before visiting the set of sites with abscissa $x_1 = 0$.

We shall compute the residence time by simulating many particles and averaging the time that each of them needs to exit, paying attention to the fact that only those particles which effectively exit through the right boundary will contribute to the average, whereas those exiting through the left boundary will be discarded.

As in the case discussed in Ref. [27] in the framework of kinetic theory, we find a surprising result: The residence time is not monotonic with respect to the geometrical parameters of the obstacle, such as its position and its size. We show also that obstacles can increase or decrease the residence time with respect to the empty strip case depending on their side lengths and on their position. In some cases, one of these parameters controls a transition from the increasing to the decreasing effect. We stress that in some cases the residence time measured in the presence of an obstacle is smaller than the one measured for the empty strip; that is to say, the obstacle is able to select those particles that cross the strip faster.

We now discuss our results for different choices of the obstacle and postpone our interpretation to the end of this section. All the details about the numerical simulations are in the figure captions. The statistical error, since negligible, is not reported in the picture.

In Fig. 2, we report the residence time as a function of the obstacle height. The obstacle is placed at the center of the strip and its width is $W = 2$ (disks), $W = 20$ (triangles), $W = 40$ (squares), and $W = 60$ (diamonds). In the case of a thin barrier, starting from the empty strip value, the residence time increases with the height of the obstacle. For a wider obstacle, an *a priori* not intuitive result is found: The dependence of the residence time on the obstacle height is not monotonic. In the case $W = 20$, starting from the empty strip value, the residence time decreases up to height 20 and then increases to values above the empty strip one. This effect is even stronger if the width of the obstacle is further increased.

In Fig. 3, we plot the residence time as a function of the obstacle width. The obstacle is placed at the center of the strip and its height is $H = 40$. When the barrier is thin, the residence time is larger than the one measured in the empty strip case, but, when the width is increased, the residence time decreases and at about 26 it becomes smaller than the empty case value. The minimum is reached at about 120 (recall that the length of the strip is $L_1 = 200$ in this simulation), and then the residence time increases to the empty strip value, which is reached when the obstacle is as long as the entire strip. This is intuitively obvious, since in such a case the lattice consists of two independent channels having the same length as the original strip.

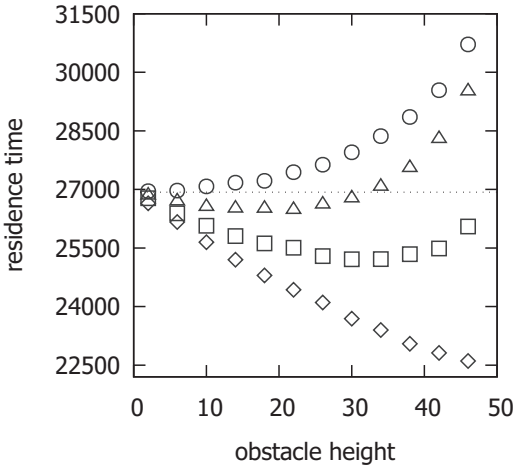

FIG. 2. Residence time vs obstacle height. The obstacle is placed at the center of the strip and its width is $W = 2$ (disks), $W = 20$ (triangles), $W = 40$ (squares), and $W = 60$ (diamonds). Simulation parameters: $L_1 = 200$, $L_2 = 50$, and total number of inserted particles 5×10^7. The total number of particles exiting through the right boundary decreases when the obstacle height is increased from 2.49×10^5 (empty strip) to 1.69×10^5 (disks), 0.99×10^5 (triangles), and 0.68×10^5 (squares), and 0.52×10^5 (diamonds) for $H = 46$. The dashed line at 26 930 represents the value of the residence time measured for the empty strip.

In Fig. 4, a centered square obstacle is considered. The residence time as a function of its side length is reported. Although small oscillations, reasonably due to numerical approximations, are visible, the behavior appears to be monotonically decreasing.

Finally, in Fig. 5, we show that—and this is really surprising—the residence time is not monotonic even as a

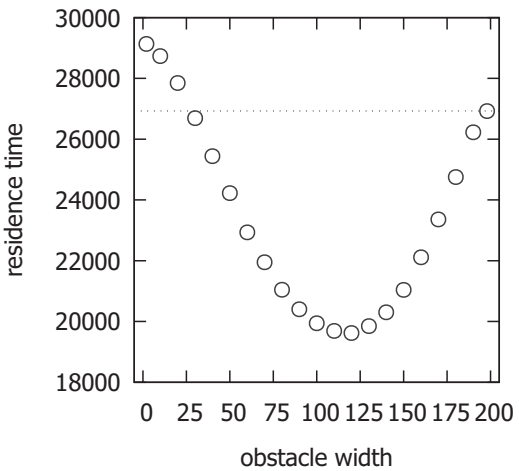

FIG. 3. Residence time vs obstacle width. The obstacle is placed at the center of the strip and its height is $H = 40$. The total number of particles exiting through the right boundary decreases when the obstacle width is increased from 2×10^5 for $W = 2$ to 0.5×10^5 for $W = 198$. The parameters of the simulation and the dashed line are as in Fig. 2.

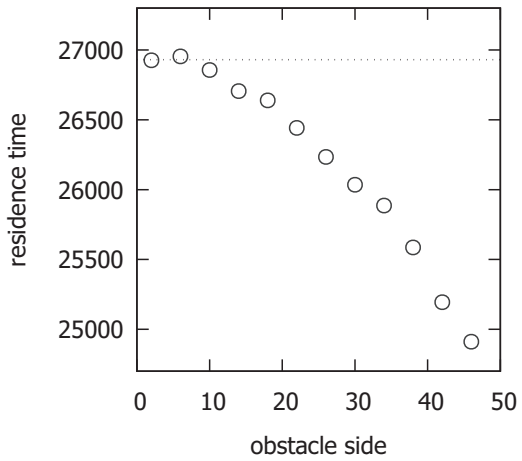

FIG. 4. Residence time vs squared obstacle side length. The squared obstacle is placed in the middle of the strip. The total number of particles exiting through the right boundary decreases when the obstacle side length is increased from 2.49×10^5 (empty strip) to 0.63×10^5 for side length equal to 46. The parameters of the simulation and the dashed line are as in Fig. 2.

function of the position of the center of the obstacle. Disks refer to a squared obstacle of side length 40, whereas triangles refer to a thin rectangular obstacle with width $W = 2$ and height $H = 40$. The integer part of the abscissa of the center of the obstacle is varied, as reported in the picture, whereas the integer part of its vertical coordinate is kept fixed to 25. In both cases, the residence time is not monotonic and attains its minimum value when the obstacle is placed in the center of the strip. In the squared obstacle case, when the abscissa of the center of the obstacle lies between 75 and 125, the residence time in the presence of the obstacles is smaller than the corresponding value for the empty strip. On the other hand,

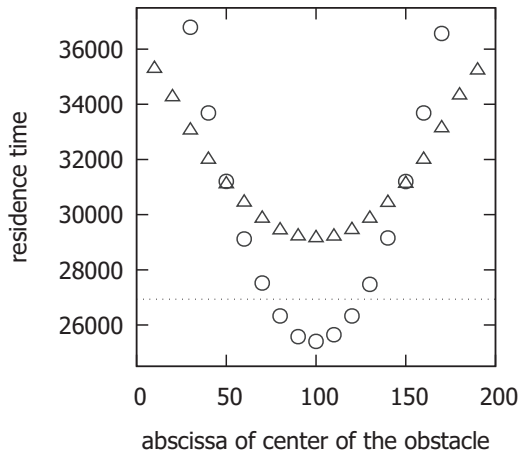

FIG. 5. Residence time vs integer part of the abscissa (first coordinate) of the geometric center of the obstacle. Disks refer to a squared obstacle with side length 40, whereas triangles refer to a rectangular obstacle with width $W = 2$ and height $H = 40$. The total number of particles exiting through the right boundary is approximately 1.24×10^5 (disks) and 2.01×10^5 (triangles) and depends poorly on the obstacle position. The parameters of the simulation and the dashed line are as in Fig. 2.

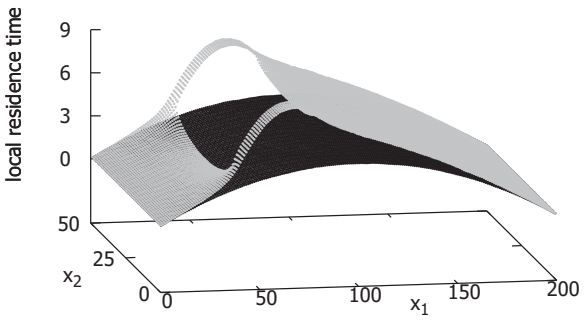

FIG. 6. Mean time spent by the walker crossing the strip in each site of the strip (local residence time) for the empty strip case (black) and in the presence of the obstacle (gray). Data are those of the experiment described by the disks in Fig. 5. The obstacle is a squared obstacles with side length 40 whose center is placed at the site with integer part of the abscissa equal to 60.

for the thin rectangular obstacle, even if the nonmonotonic behavior is found, the residence time is always larger than in the empty strip case. This fact is consistent with the results plotted in Fig. 2.

The results that we found in the numerical experiments reported in Figs. 2–5 can be summarized as follows: The residence time strongly depends on the obstacle geometry and position. In particular, it seems that large centered obstacles favor the selection of particles crossing the strip more quickly than in the empty strip case.

In order to explain our observations, following Ref. [27], we partition the strip into three parts: the rectangular region on the left of the obstacle, the rectangular region on the right of the obstacle, and the remaining central part containing the obstacle. As we will see later, the residence time behavior is a consequence of two effects in competition: The total time spent by the particles in the channels between the obstacle and the horizontal boundary is smaller than the total time spent in the central part of the strip in the empty case. On the contrary, the total time spent both in the left and right parts of the strip is larger than that in the empty case. Both these two effects can be explained remarking that, when the obstacle is present, it is more difficult for the walker to enter the central region of the strip, namely, one of the channels flanking the obstacle. The total residence time trend depends on which of the two effects dominates the dynamics of the walker.

To illustrate our interpretation of the phenomenon, we describe in detail the walker behavior referring to the experiment associated with the disks in Fig. 5. In Fig. 6, we plot the mean time spent by the walker crossing the strip in each site of the strip. This quantity will be addressed as the *local residence time*. The gray surface in the picture refers to the obstacle case, whereas the black surface is related to the empty strip case. The data in the picture have been collected in the case in which the center of a squared obstacle with side length 40 is the point such that the integer parts of its coordinates are (60,25). The graph shows that on average in each site of the strip the particle spends a time larger than the time it spends at the same site in the empty strip case. This seems to be in contrast with the fact that the (total) residence time in the strip can be smaller when the obstacle is present. Indeed, this can

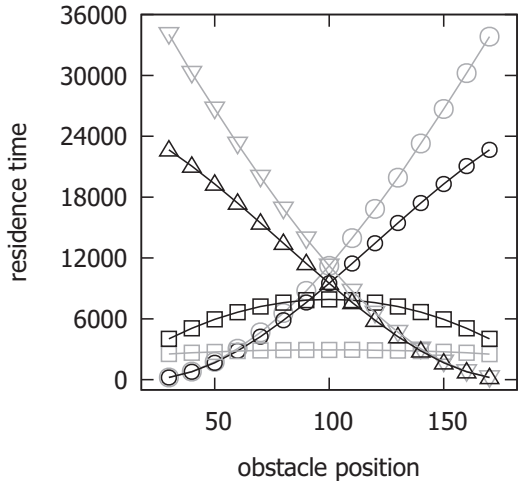

FIG. 7. Total residence time in the left (circles), central (squares), and right (triangles) parts of the strip in the presence of the obstacle (gray) and in the empty strip case (black). The experiment associated with the disks in Fig. 5 is considered.

happen since the sites of the strip falling in the obstacle region are never visited by the walker. It can then happen that the sum of the local residence times associated with sites in the central part of the strip in the presence of the obstacle is smaller than the same sum computed in the empty strip case.

Results in Fig. 6 can be interpreted as follows. The local residence times in the left and right regions are larger with respect to the empty case since for the particle it is more difficult to access the central region and, thus, it will spend more time in the lateral parts of the strip. On the other hand, once the particle enters into one of the two central channels, it will take on average the same time to get back to one of the two lateral parts of the strip as it would take in the absence of the obstacle. But, since the number of the available sites in the central part is smaller when the obstacle is present, the local residence time will be larger.

Figure 6 gives some new insight in the motion of the walker, but it is not sufficient to explain the residence time behavior discussed above. In order to get some insight into this, we compute the respective times spent by the particle in the left, central, and right regions of the strip. This is done in Fig. 7, where data referring to the experiment associated with the disks in Fig. 5 are reported. First, one should note that the total residence time in the left and right parts of the strip are increased when the obstacle is present; this is due to the fact that for the particle it is more difficult to enter the central part when the obstacle is present. Moreover, precisely for the same reason, the trajectory of the walker from its starting point to its exit from the strip will visit the channels in the central region of the strip less than the number of times the particle visits the central region of the strip in the empty strip case. Thus, the residence time in the central part of the strip is smaller when the obstacle is present.

Hence, the behavior of the (total) residence time data reported as disks in Fig. 5 can be explained as follows: If the center of the obstacle is close to the left boundary (say, its abscissa is smaller than 75), then the effect in the right region of the strip dominates the one in the central region and the (total) residence time is increased (the effect in the left region in this case is negligible). On the other hand, if the center of the obstacle is close to the center of the strip (say, its abscissa is between 75 and 125), then the effect in the central region dominates and the (total) residence time is decreased. Finally, if the center of the obstacle is close to the right boundary (say, its abscissa is larger than 125), then the effect in the left region of the strip dominates the one in the central region and the (total) residence time is increased (the effect in the right region in this case is negligible).

The behavior of the residence time in connection with all the experiments illustrated in Figs. 2–5 can be explained similarly.

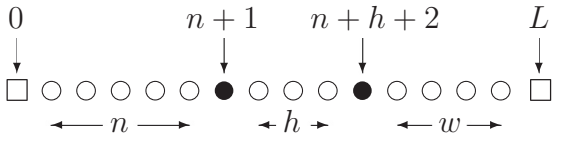

FIG. 8. Representation of the lattice on which the 1D model is defined. Open and solid circles respectively represent regular and special (defect) sites. The two squared boxes represent the two boundary absorbing sites. Recall that $L = n + h + w + 3$.

III. THE 1D MODEL

In this section, we propose a one-dimensional reduction of the problem based on a symmetric simple random walk with two defect sites. We actually prove that the behaviors of the 1D system are similar to those discussed above and that the Monte Carlo data are fully supported by exact analytical computations.

We consider a simple random walk on $\{0,1,\ldots,L\}$, i.e., the set $[0,L]\cap\mathbb{Z}$. The sites 0 and L are absorbing, so that when the particle reaches one of these two sites the walk is stopped. All the sites $1,\ldots,L-1$ are *regular* excepted for two sites called *defect* or *special* sites (see Fig. 8). The *first* or *left* defect site is the site $n+1$ and the *second* or *right* defect site is the site $n+h+2$, with the parameters n and h that can take the value $n\in\{1,2,\ldots,L-5\}$ and $h\in\{1,2,\ldots,L-n-4\}$. The parameters n and h are chosen in such a way that the left defect site cannot be 1, the right defect site cannot be $L-1$, and there is at least one regular site separating the two defect sites. The number of regular sites on the left of the left defect site is n and the number of regular sites in the region between the two defect sites is h. We let $w = L-(n+h+3)$ be the number of regular sites on the right of the right defect site.

At each unit of time, the walker jumps to a neighboring site according to the following rule: If it is on a regular site, then it performs a simple symmetric random walk. If it is at the left defect site, then with probability λ it jumps to the right, with probability $1-\lambda-\epsilon$ it jumps to the left, and with probability ϵ it does not move. If it is at the right defect site, then with probability λ it jumps to the left, with probability $1-\lambda-\epsilon$ it jumps to the right, and with probability ϵ it does not move. Here, $\lambda\in(0,1)$ and $\epsilon\in[0,1)$.

The array $1,\ldots,L-1$ will be called the *lane*. The sites 0 and L will be, respectively, called the *left* and *right exits* of the lane.

This 1D model is a toy model for the 2D system that we have discussed in Sec. II. Indeed, the left defect site $n+1$ mimics the sites in the first column of the 2D strip on the left of the obstacle: The 2D walker in such a column has a probability to move to the right that is smaller than the probability to move to the left. Similarly, the right defect site $n+h+1$ mimics the sites in the first column to the right of the obstacle. Let us stress that the sites $n+1+1,\ldots,n+h$ are regular, since when the 2D walker enters one of the two channels flanking the obstacle its probability to move to the right is equal to that to move to the left.

In this framework, the residence time is defined by starting the walk at site 1 and computing the typical time that the particle takes to reach the site L provided the walker reaches L before 0. More precisely, we let x_t be the position of the walker at time t and denote by $\mathbb{P}_k$ and $\mathbb{E}_k$ the probability associated to the trajectories of the walk and the related average operator for the walk started at $x_0 = k$ with $k = 1,\ldots,L-1$. We let T_i be the *first hitting time to* i, namely, the first time at which the trajectory of the walk reaches the site i, with the convention that $T_i = \infty$ if the trajectory does not reach the site i. The main quantity of interest is the *residence time* or *total residence time*

$$R = \mathbb{E}_1[T_L | T_L < T_0] = \sum_{t=1}^{\infty} t\,\mathbb{P}_1[T_L = t | T_L < T_0] \quad . \quad (3.1)$$

Note that the residence time is defined for the walk started at $x_0 = 1$ and the average is computed conditioning to the event $T_L < T_0$, namely, conditioning to the fact that the particle exits the lane through the right exit.

As in the 2D case discussed in Sec. II, we shall compute numerically the residence time by simulating many particles and averaging the time that each of them takes to exit through the right ending point, discarding all the particles exiting through the left ending point. But we stress that in this 1D model it is also possible to compute exactly the residence time. In this section, we shall discuss our findings and in each plot the solid lines will represent the exact result which will be discussed in Sec. IV.

We now discuss our results for different choices of the parameter which are the analog of the cases considered in Sec. II for the 2D model. All the details about the numerical simulations are in the figure captions. The statistical error, since negligible, is not reported in the picture. We carry out the simulations with the following choice of the parameters:

$$\epsilon = \tfrac{1}{2}p \quad \text{and} \quad \lambda = \tfrac{1}{2}(1-p) \quad (3.2)$$

with $p \in [0,1)$, so that $\epsilon \in [0,1/2)$ and $\lambda \in (0,1/2]$. Note that with such a choice the probability to move left (right) for the particle sitting at the left (right) defect site is $1-\lambda-\epsilon = 1/2$. Note that for p equal zero we recover the symmetric simple random walk, which mimics the 2D empty strip.

The case reported in Fig. 9 is the analog of the case discussed in Fig. 2 in the 2D setting. Indeed, the residence time is plotted as a function of the parameter p increasing from 0 to 0.99 and this mimics the increase of the height of the obstacle considered in Fig. 2. Moreover, the two defect sites are symmetric with respect to the middle point of the lane and the number of regular sites between them is chosen equal to 2, 20, 40, and 60, mimicking the different obstacle widths considered in Fig. 2.

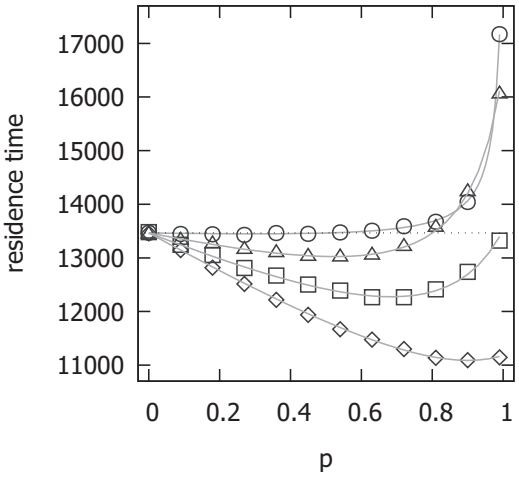

FIG. 9. Residence time vs p. Simulation parameters: total number of inserted particles 5×10^7, $L = 201$, $n = 98$ and $h = 2$ (disks), $n = 89$ and $h = 20$ (triangles), $n = 79$ and $h = 40$ (squares), and $n = 69$ and $h = 60$ (diamonds). The total number of particles exiting through the right exit decreases when p grows from 2.48×10^5 (no defect is present, namely, $p = 0$) to 1×10^5 (disks), 0.22×10^5 (triangles), 0.12×10^5 (squares), and 0.08×10^5 (diamonds) for $p = 0.99$. The dashed line at 13466 represents the value of the residence time measured in absence of defect sites ($p = 0$). The solid line is the exact solution.

The data show a behavior similar to that reported in Fig. 2 in the 2D case: In the case $h = 2$ (the defect sites are close to each other) the residence time increases with p. For a wider obstacle, the nonmonotonic behavior is recovered. In the case $h = 20$, starting from the empty strip value, the residence time decreases up to $p \sim 0.55$ and then it increases to values above the $p = 0$ case. This effect is even stronger if p is further increased.

The case reported in Fig. 10 is the analog of the case discussed in Fig. 3 in the 2D setting. Indeed, the residence

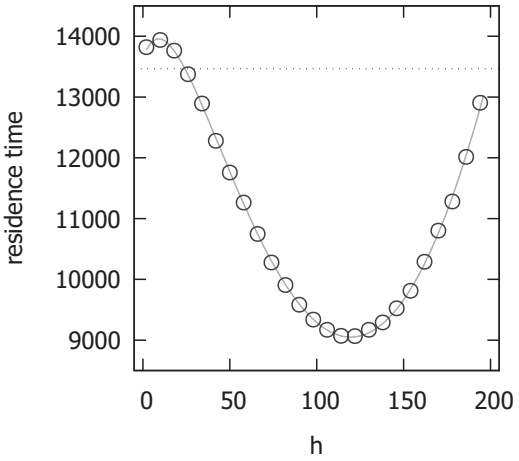

FIG. 10. Residence time vs h (even) for $p = 0.84$, $L = 201$, $n = (L-h-3)/2$, and total number of inserted particles 5×10^7. The dashed and the solid lines are as in Fig. 9. The total number of particles exiting through the right exit decreases when h is increased from 2.31×10^5 for $h = 2$ to 0.41×10^5 for $h = 194$.

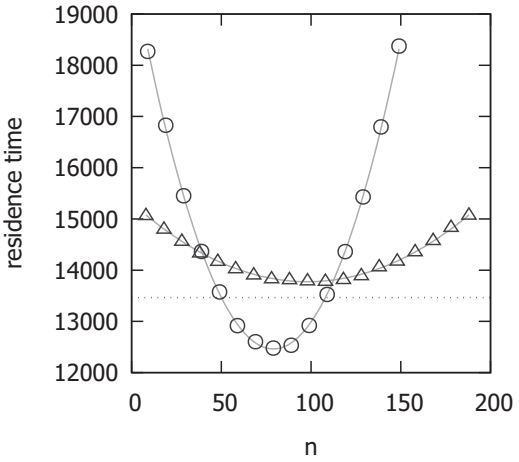

FIG. 11. Residence time vs n for $p = 0.84$, $L = 201$, $h = 40$ (disks), $h = 2$ (triangles), and total number of inserted particles 5×10^7. The dashed and the solid lines are as in Fig. 9. The total number of particles exiting through the right exit is approximately equal to 1.2×10^5 (disks) and 2.3×10^5 (triangles).

time is plotted as a function of the parameter h increasing from 2 to 198 with the two defect sites symmetric with respect to the middle point of the lane. This case mimics the increase of the width of the centered rectangular obstacle reported in Fig. 3. When h is small, the residence time is larger than the one measured for $p = 0$, but, when h is increased, the residence time decreases and at about 25 it becomes smaller than the $p = 0$ case. The minimum is reached at about 120 (recall the lane is long 201 sites in this simulation), and then the residence time increases toward the $p = 0$ value.

In this 1D setting, it is not really clear how to construct an analog for the experiment in Fig. 4, where a squared centered obstacle was considered. On the other hand, the case reported in Fig. 11 is the analog of the case discussed in Fig. 5 in the 2D setting. Indeed, the residence time is plotted as a function of the parameter n in the two cases $h = 40$ (disks) and $h = 2$ (triangles). This case mimics the increase of the abscissa of the center of the obstacle reported in Fig. 5. In both cases, the residence time is nonmonotonic and attains its minimum value when the defect sites are symmetric with respect to the center of the lane. In the $h = 40$ case, when n lies approximately between 50 and 110, the residence time is smaller than the corresponding value for the case $p = 0$. On the other hand, for $h = 2$, even if the nonmonotonic behavior is recovered, the residence time is always larger than the one measured in the $p = 0$ case. This fact is consistent with the results plotted in Fig. 9.

The exact computation of the residence time allows us to fully depict the residence time behavior as a function of the parameters of the system. In Fig. 12, we consider the defect sites to be symmetric with respect to the middle point of the lane. The residence time as a function of h and p is plotted. Note that for $p = 0$ the random walk is symmetric, i.e., no defect site is present, and the residence time value in absence of special sites is recovered. Note also that for h fixed to 2, 20, 40, and 60 and varying p, the behaviors described by Fig. 9 are clearly visible, as well as that one of Fig. 10 for p fixed and varying

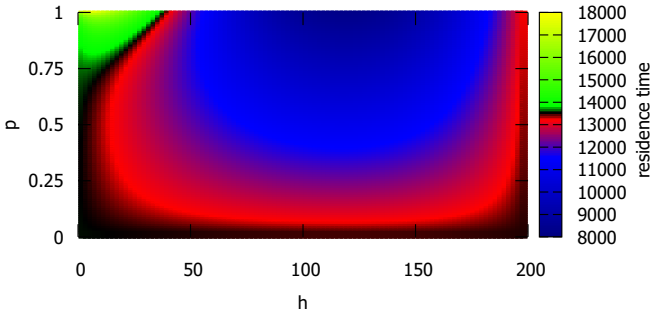

FIG. 12. Residence time as a function of h and p, for $L = 201$ and defect sites symmetric with respect to the middle point of the lane. For $p = 0$, the residence time is 13 466 (absence of defect sites).

h. In Fig. 13, the residence time is evaluated as a function of n and h, for a fixed value of $p = 0.9$. Note that, since $L = n + h + w + 3$, for fixed L the distance h can vary only from 1 to $L - n - 4$. For fixed h, the dependence of the residence time on the positions of the first defect, i.e., the dependence on n, is clearly understood and it is consistent with the cases of fixed h equals to 2 and 40 respectively, depicted in Fig. 11.

In order to explain these observations, in a manner similar to what we did in the 2D case and in Ref. [27], we partition the lane into three parts: the part of the lane on the left of the left defect (left region), the part of the lane between the two defect sites (central region), and the part of the lane on the right of the right defect (right region). As in the 2D case, the residence time behavior is a consequence of two effects in competition: The total time spent by the particles in the central region is less than the total time spent in the same region in the absence of defect sites ($p = 0$). On the contrary, the total time spent both in the left and right regions is longer than the time spent there in the $p = 0$ case. Both these effects can be explained by remarking that, in the presence of defect sites, it is more difficult for the walker to enter the central region of the lane. The total residence time trend depends on which of the two effects dominates the dynamics of the walker.

These remarks are illustrated in Fig. 14, where data referring to the experiment associated with the disks in Fig. 11 are reported. Again, one notes that the total residence time in the left and right regions of the lane is increased when the defect sites are present, which is due to the fact that for the particle

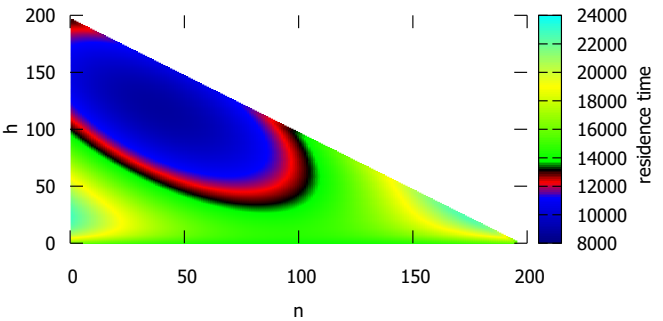

FIG. 13. Residence time as a function of n and h, for $L = 201$ and $p = 0.9$. Recall that in the case of symmetric random walk (no defect sites), the residence time is 13 466.

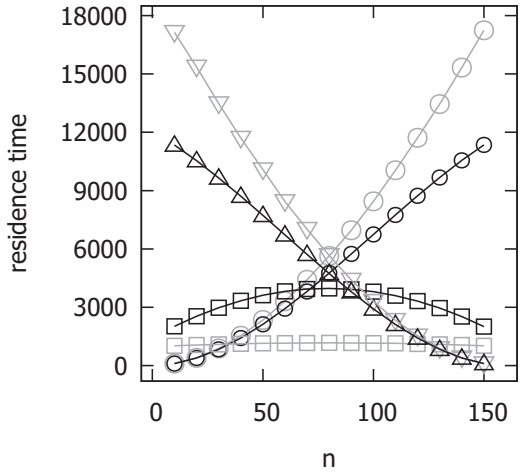

FIG. 14. Total residence time in the left (circles), central (squares), and right (triangles) regions of the lane in the presence of the defect sites (gray) and in the $p = 0$ case (black). The experiment associated with the disks in Fig. 11 is considered.

it is more difficult to enter the central region in such a case. Moreover, precisely for the same reason, the trajectory of the walker from its starting point 1 to its exit from the lane will visit the central region of the lane less than the number of times that the particle visits such a region in the $p = 0$ case. Thus, the residence time in the central region is smaller in the presence of the defect site. Finally, like what we did in the 2D case, the results in Fig. 14 allow a complete interpretation of the residence time behavior depicted by the disks in Fig. 11 (note that the maximum value of the variable n for the disks in Fig. 11 is 150).

IV. ANALYTIC RESULTS

In this section, we derive exact, though not explicit, expressions for the residence time defined in Sec. III. To compute the residence time, we shall make use of the following result on a five-state chain: The states are S, A, B, C, and D. The jump probabilities are as depicted in the Fig. 15 and the chain is started at time 0 in B. We prove that the probability Q_k, with $k \geqslant 1$, for the chain to reach D before S and return $k-1$ times to the site B before reaching D is

$$Q_k = p_B p_C [r_B + q_B p_A + p_B q_C]^{k-1}, \tag{4.3}$$

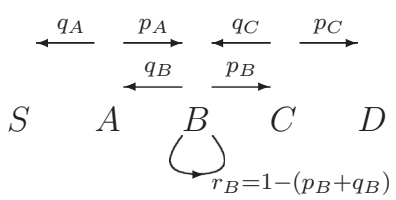

FIG. 15. Schematic representation of the five-state chain model.

where $r_B = 1 - (p_B + q_B)$. Indeed,

$$Q_k = p_B p_C \sum_{r=0}^{k-1} \binom{k-1}{r} (p_B q_C)^{k-1-r} \times \sum_{s=0}^{r} \binom{r}{s} (q_B p_A)^s (r_B)^{r-s},$$

where r counts the number of times that, starting from B, the chain either jumps to A or it stays in B and s counts the number of times that starting from B it jumps to A. Equation (4.3) is then proven by using the binomial theorem.

We now consider again the 1D walk defined in Sec. III. To compute the residence time, we introduce the *local times*, i.e., the time spent by a trajectory at site i defined as

$$\tau_i = |\{t : t > 0 \text{ and } x_t = i\}| \tag{4.4}$$

for any $i = 1, \ldots, L-1$, where $|A|$ denotes the cardinality of the set A. Provided T_L is finite, we have that

$$T_L = \sum_{i=1}^{L-1} \tau_i. \tag{4.5}$$

Hence the residence time R defined in (3.1) can be expressed as

$$R = \sum_{i=1}^{L-1} \mathbb{E}_1[\tau_i | T_L < T_0] \tag{4.6}$$

and for all $i \in \{1, \ldots, L-1\}$

$$\mathbb{E}_1[\tau_i | T_L < T_0] = \frac{\mathbb{P}_1[T_i < T_0]}{\mathbb{P}_1[T_L < T_0]} \frac{p_B p_C}{[1 - (r_B + q_B p_A + p_B q_C)]^2}, \tag{4.7}$$

where we defined the quantities

$$\begin{aligned} p_A &= \mathbb{P}_{i-1}(T_i < T_0), \quad q_A = \mathbb{P}_{i-1}(T_0 < T_i), \\ p_B &= \mathbb{P}_i(x_1 = i+1), \quad q_B = \mathbb{P}_i(x_1 = i-1), \\ p_C &= \mathbb{P}_{i+1}(T_L < T_i), \quad q_C = \mathbb{P}_{i+1}(T_i < T_L). \end{aligned} \tag{4.8}$$

Note that $p_A + q_A = 1$, $p_B + q_B + r_B = 1$, and $p_C + q_C = 1$. Indeed, we have

$$\mathbb{E}_1[\tau_i | T_L < T_0] = \sum_{k=1}^{\infty} k \mathbb{P}_1[\{i \text{ visited } k \text{ times}\} | \{T_L < T_0\}]$$

and, using the definition of conditional probability and the Markov property,

$$\begin{aligned} &\mathbb{E}_1[\tau_i | T_L < T_0] \\ &= \sum_{k=1}^{\infty} k (\mathbb{P}_1[\{T_i < T_0\}] / \mathbb{P}_1[\{T_L < T_0\}]) \\ &\quad \times \mathbb{P}_i[\{T_L < T_0\} \cap \{k-1 \text{ returns to } i\}]. \end{aligned}$$

The last probability appearing in the above expression is nothing but the quantity Q_k defined for the five-state chain with the jump probabilities defined as in (4.8). Finally, (4.7)

follows by noting that

$$\sum_{k=1}^{\infty} k Q_k = \frac{p_B p_C}{[1-(r_B + q_B p_A + p_B q_C)]^2}.$$

Our strategy to compute the residence time is the following: For any $i = 1, \ldots, L-1$ we shall compute $\mathbb{E}_1[\tau_i | T_L < T_0]$, identifying the correct values of p_A, q_A, p_B, q_B, p_C, and q_C to be used, whose definition depends on the choice of the site i. Finally, the sum (4.6) will provide us with the residence time.

A. Residence time in the symmetric case

In the symmetric case, that is $\epsilon = 0$ and $\lambda = 1/2$, by using the gambler's ruin result [a situation in which each gambler (player) can win or lose a certain sum (amount) from his or her adversaries], we have that

$$\mathbb{P}_1[T_0 < T_L] = \frac{L-1}{L} \tag{4.9}$$

and

$$\mathbb{P}_1[T_L < T_0] = \frac{1}{L}. \tag{4.10}$$

This is a very classical problem in probability theory which can be found in any probability textbook; see, for example, Ref. [28, paragraphs 2 and 3, Chapter XIV].

The computation of the residence time, which, in the gambler language, is the average duration of the game conditioned to the fact that the gambler wins, is not immediate. We use the formulas (4.6)–(4.8) proven above by defining suitably the five-state chain jump probabilities. More precisely, $p_A = (i-1)/i$ is given by (4.9) with the initial point 1 replaced by $i-1$ and L replaced by i, $q_A = 1/i$ is similarly given by (4.10), $p_B = q_B = 1/2$ (and hence $r_B = 0$), $p_C = 1/(L-i)$ is given by (4.10) with the initial point 1 replaced by $i+1$ and L replaced by $L-i$, and $q_C = (L-i-1)/(L-i)$ is given similarly by (4.9). Moreover, since from (4.9) it also follows that $\mathbb{P}_1[T_L < T_0] = 1/L$ and $\mathbb{P}_1[T_i < T_0] = 1/i$, from (4.7) a straightforward computation yields

$$\mathbb{E}_1[\tau_i | T_L < T_0] = \frac{2}{L}(Li - i^2)$$

and, computing the sum in (4.6), we finally have

$$R = \tfrac{1}{3}(L-1)(L+1). \tag{4.11}$$

In Fig. 16, the numerical estimate of the residence time in this symmetric case is compared to the exact result (4.11). It is interesting to remark that the mean time that a symmetric walk started at 0 needs to reach either $-L$ or $+L$ is L^2. This time can be computed as the average duration of the gambler's game. Thus, conditioning the particle to exit through the right end point decreases by a multiplicative factor the mean time that the particle needs to reach the distance L from the starting point, but it does not change the diffusive dependence on the length L of the lane.

B. Crossing probability in the general case

We now come back to the general 1D model introduced in Sec. III. As a first step in the residence time computation, we have to calculate the *crossing probability* $\mathbb{P}_1[T_L < T_0]$ which

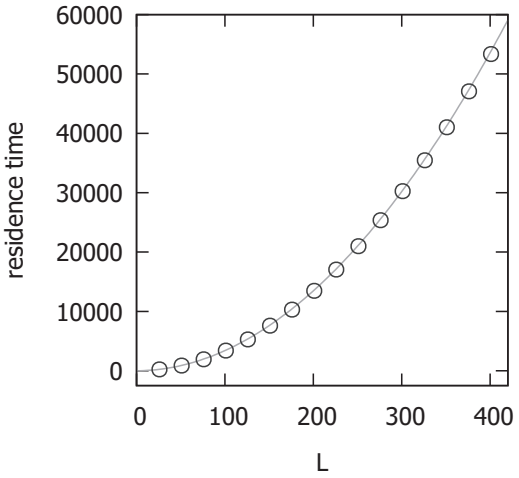

FIG. 16. Residence time vs L for the lane with no singular sites (symmetric case). The solid line is the exact solution (4.11), whereas circles are the average results of a Monte Carlo simulation with 5×10^8 particles started at the site 1.

appears at the denominator in (4.7). We first note that, by using repeatedly the Markov property, one gets

$$\mathbb{P}_1[T_0 < T_L] = 1 - p_1 p_2 p_3 p_4 p_5 \tag{4.12}$$

and, as a consequence

$$\mathbb{P}_1[T_L < T_0] = p_1 p_2 p_3 p_4 p_5, \tag{4.13}$$

where

$$p_1 = \mathbb{P}_1[T_0 > T_{n+1}],\ p_2 = \mathbb{P}_{n+1}[T_0 > T_{n+2}],$$
$$p_3 = \mathbb{P}_{n+2}[T_0 > T_{n+h+2}],\ p_4 = \mathbb{P}_{n+h+2}[T_0 > T_{n+h+3}],$$
$$p_5 = \mathbb{P}_{n+h+3}[T_0 > T_L].$$

The probabilities $p_1, \ldots, p_5$ can be computed explicitly and the remaining part of this section is devoted to the computation of these quantities. For p_1, one has to use (4.10) with L replaced by $n+1$ to deduce that

$$p_1 = \frac{1}{n+1}. \tag{4.14}$$

To compute p_2, we first note that, once the particle is in n, the probability to come back to $n+1$ before reaching 0 is equal to $n/(n+1)$, as it follows by using (4.9) with the initial point 1 replaced by n and L replaced by $n+1$. Hence,

$$p_2 = \sum_{r=0}^{\infty} \sum_{k=0}^{r} \binom{r}{k} \left[(1-\varepsilon-\lambda)\frac{n}{n+1}\right]^{r-k} \varepsilon^k \lambda,$$

where r counts the number of times that, starting from $n+1$, the walker either jumps to n or it stays in $n+1$ and k counts the number of times that the walker stays in $n+1$. Using the binomial theorem, we get

$$p_2 = \frac{\lambda}{1-[(1-\varepsilon-\lambda)n/(n+1)+\varepsilon]}. \tag{4.15}$$

In order to compute p_3, note that, using (4.9) and (4.10) with initial point $n+2$ and replacing L with $h+1$, one has $\mathbb{P}_{n+2}[T_{n+1} < T_{n+h+2}] = h/(h+1)$ and

$\mathbb{P}_{n+2}[T_{n+h+2} < T_{n+1}] = 1/(h+1)$. Hence,

$$p_3 = \frac{1}{h+1}\sum_{k=0}^{\infty}\left(\frac{h}{h+1}\right)^k p_2^k = \frac{1}{1+h(1-p_2)}\,, \tag{4.16}$$

where k counts the number of times that, starting from $n+2$, the walker reaches $n+1$ before $n+h+2$.

To compute p_4, we first need to calculate $\xi = \mathbb{P}_{n+h+1}[T_0 > T_{n+h+2}]$. Starting from $n+h+1$, the probability to reach $n+h+2$ before $n+1$ is $\mathbb{P}_{n+h+1}[T_{n+h+2} < T_{n+1}] = h/(h+1)$, where we used (4.9) with initial point $n+h+1$ and L replaced by $h+1$. Hence, $\mathbb{P}_{n+h+1}[T_{n+1} < T_{n+h+2}] = 1/(h+1)$. Thus,

$$\xi = \frac{h}{h+1} + \frac{1}{h+1}p_2\frac{1}{h+1}\sum_{k=0}^{\infty}\left(p_2\frac{h}{h+1}\right)^k,$$

where k counts the number of times that the walker returns to $n+1$ after having visited it for the first time. We have also used that $\mathbb{P}_{n+2}[T_{n+1} < T_{n+h+2}] = h/(h+1)$. With some algebra, we find the expression

$$\xi = \frac{p_2 + h(1-p_2)}{1+h(1-p_2)}. \tag{4.17}$$

Now, we have all the ingredients to compute p_4. Indeed,

$$p_4 = (1-\varepsilon-\lambda)\left[\sum_{r=0}^{\infty}\sum_{k=0}^{r}\binom{r}{k}\varepsilon^k(\lambda\xi)^{r-k}\right],$$

where $r-k$ counts the number of times that the walker starting from $n+h+2$ jumps to $n+h+1$ and where k counts the number of times that the walker stays at $n+h+2$. A simple calculation provides the result

$$p_4 = \frac{1-\varepsilon-\lambda}{1-(\lambda\xi+\varepsilon)}. \tag{4.18}$$

Finally, to compute p_5 we remark that $\mathbb{P}_{n+h+3}[T_L < T_{n+h+2}] = 1/(w+1)$ and $\mathbb{P}_{n+h+3}[T_{n+h+2} < T_L] = w/(w+1)$, as it can be deduced by (4.10) and (4.9) by using as initial point the point $n+h+3$ and replacing L by $w+1$. Then,

$$p_5 = \frac{1}{w+1}\sum_{k=0}^{\infty}\left(\frac{w}{w+1}p_4\right)^k = \frac{1}{1+w(1-p_4)}. \tag{4.19}$$

Finally, plugging Eqs. (4.14)–(4.19) into Eq. (4.13), we find the expression

$$\mathbb{P}_1[T_L < T_0] = \frac{\lambda}{(1+h)(1-\varepsilon-2\lambda)+\lambda L} \tag{4.20}$$

for the probability that the particle which started at the site 1 reaches L before visiting 0. It is interesting to remark that in the case $\varepsilon = 0$ and $\lambda = 1/2$ the expression (4.10) valid in the symmetric case is recovered.

C. Residence time in the presence of defects

The last step, necessary to complete our algorithm to compute the residence time, is that of listing the expression that must be used for the probabilities (4.8) for the different choices of i on the lattice. In this last section, in order to get simpler formulas, we focus on the case that has been studied numerically; that is to say, we choose the parametrization (3.2). First of all, we note that the expression (4.20) of the probability that the particle started at the site 1 reaches L before visiting 0 simplifies to

$$\mathbb{P}_1[T_L < T_0] = \frac{1-p}{p(1+h)+(1-p)L}. \tag{4.21}$$

The site i in the lattice can be chosen in nine possible different ways: in the bulk of the three regions on the left, between and on the right of the defect sites, as one of the four sites neighboring the defects, and as one of the two defect sites. We list only five cases; the remaining four can be deduced by exchanging the role of the parameters n and w. Note that we shall only list either p_A or q_A and p_C or q_C; the missing parameter can be deduced by the equations $p_A + q_A = 1$ and $p_C + q_C = 1$.

Case $1 \leqslant i \leqslant n-1$. First note that $\mathbb{P}_1[T_i < T_0] = 1/i$ is given by (4.10) with initial site 1 and L replaced by i. Moreover, $p_A = (i-1)/i$ follows from (4.9) with initial site $i-1$ and L replaced by i. We trivially have that $p_B = q_B = 1/2$. Finally, $p_C = (1-p)/[p(1+h)+(1-p)(L-i)]$ follows from (4.21) with initial site $i+1$ and L replaced by $L-i$.

Case $i = n$. First note that $\mathbb{P}_1[T_i < T_0] = 1/n$ is given by (4.10) with initial site 1 and L replaced by n. Moreover, $p_A = (n-1)/n$ follows from (4.9) with initial site $n-1$ and L replaced by n. We trivially have that $p_B = q_B = 1/2$. Finally, we note that q_C has the same structure as p_4; thus, by exchanging the role of n and w, from (4.15), (4.17), and (4.19) we have that $q_C = 1/[2-p-(1-p)\zeta]$ where

$$\zeta = \frac{\pi + h(1-\pi)}{1+h(1-\pi)} \quad \text{and} \quad \pi = \frac{1-p}{2-p-\frac{w}{w+1}}\,. \tag{4.22}$$

Case $i = n+1$. First note that $\mathbb{P}_1[T_i < T_0] = 1/(n+1)$ is given by (4.10) with initial site 1 and L replaced by $n+1$. Moreover, $p_A = n/(n+1)$ follows from (4.9) with initial site n and L replaced by n. We trivially have that $p_B = (1-p)/2$ and $q_B = 1/2$. Finally, we note that q_C has the same structure as ξ; thus, by exchanging the role of n and w, from (4.17) we have that $q_C = \zeta$. See (4.22).

Case $i = n+2$. First note that $\mathbb{P}_1[T_i < T_0] = p_1p_2$, and hence, using (4.14) and (4.15), an easy computation yields $\mathbb{P}_1[T_i < T_0] = (1-p)/\{(n+1)[2-p-n/(n+1)]\} = (1-p)/[2+n-p(n+1)]$ since, with the parametrization that we are adopting in this section,

$$p_2 = \frac{1-p}{2-p-n/(n+1)}.$$

Moreover, $p_A = p_2$ by definition and $p_B = q_B = 1/2$. Finally, we note that q_C has the same structure as ξ with h replaced by $h-1$. Thus, by exchanging the role of n and w, from (4.17) we have that $q_C = [\pi + (h-1)(1-\pi)]/[1+(h-1)(1-\pi)]$, with π defined in (4.22).

Case $n+3 \leqslant i \leqslant n+h$. First note that $\mathbb{P}_1[T_i < T_0] = p_1p_2\bar{p}_3$, where $\bar{p}_3$ has the structure of p_3 with h replaced by $i-(n+2)$. Hence (4.16) gives us $\mathbb{P}_1[T_i < T_0] = (p_1p_2)/[1+(i-n-2)(1-p_2)]$ with p_1 and p_2 as in the previous case. Moreover, p_A has the same structure as ξ with h replaced by $i-n-2$ so $p_A = [p_2 + (i-n-2)(1-p_2)]/[1+(i-n-2)(1-p_2)]$ and $p_B = q_B = 1/2$. Finally, we note that q_C has the same structure as ξ with h replaced by $n+h+1-i$. Thus, by exchanging the role of n and w, from (4.17) we have that $q_C =$

$[\pi + (n + h + 1 - i)(1 - \pi)]/[1 + (n + h + 1 - i)(1 - \pi)]$, with π defined in (4.22).

V. CONCLUSIONS

We have studied in detail the effect of an obstacle in a 2D strip on the flux of particles performing a simple symmetric random walk. We have found that, due to purely geometrical effects, the typical time that a particle entered in strip through the left boundary and leaving the system through the right boundary has a complex dependence on the geometrical parameters of the obstacle. In particular, we stress that we found nonmonotonic behaviors as a function of width and position of a sufficiently large obstacle. A natural intriguing question is that of understanding if such a phenomenon can give raise to uphill currents [29]. These phenomena have been interpreted in terms of the total time that the particles spend in each of the three regions of the strip in which the obstacle naturally partitions the lattice: the one on its left, the one on its right, and the channels between the obstacle and the horizontal boundary. Finally, we have studied numerically and analytically a 1D model mimicking the 2D random walk and we have found similar results. One of the most relevant aspect has been to express the residence time in terms of conditional expectation of the duration of a random walk in the presence of singular sites (see Ref. [30] for the conditional problem with no singular sites). In this case, we have been able to develop a complete analytical computation and to compare our numerical results to the exact solution.

ACKNOWLEDGMENT

E.N.M.C. thanks R. van der Hofstad for very useful discussions.

[1] E. Cristiani and D. Peri, Appl. Math. Model. **45**, 285 (2017).
[2] E. Cristiani, F. S. Priuli, and A. Tosin, SIAM J. Appl. Math. **75**, 605 (2015).
[3] M. J. Saxton, Biophys. J. **66**, 394 (1994).
[4] F. Höfling and T. Franosch, Rep. Prog. Phys. **76**, 046602 (2013).
[5] M. A. Mourão, J. B. Hakim, and S. Schnell, Biophys. J. **107**, 2761 (2017).
[6] A. J. Ellery, M. J. Simpson, S. W. McCue, and R. E. Baker, J. Chem. Phys. **140**, 054108 (2014).
[7] K. To, P. Y. Lai, and H. K. Pak, Phys. Rev. Lett. **86**, 71 (2001).
[8] I. Zuriguel, A. Garcimartín, D. Maza, L. A. Pugnaloni, and J. M. Pastor, Phys. Rev. E **71**, 051303 (2005).
[9] F. Alonso–Marroquin, S. I. Azeezullah, S. A. Galindo-Torres, and L. M. Olsen-Kettle, Phys. Rev. E **85**, 020301 (2012).
[10] I. Zuriguel, A. Janda, A. Garcimartín, C. Lozano, R. Arévalo, and D. Maza, Phys. Rev. Lett. **107**, 278001 (2011).
[11] D. Helbing, Rev. Mod. Phys. **73**, 1067 (2001).
[12] N. Bellomo and C. Dogbé, SIAM Rev. **53**, 409 (2011).
[13] D. Helbing, P. Molnár, I. J. Farkas, and K. Bolay, Environ. Plan. B **28**, 361 (2001).
[14] D. Helbing, I. Farkas, P. Molnàr, and T. Vicsek, in *Pedestrian and Evacuation Dynamics*, edited by M. Schreckenberg and S. D. Sharma (Springer, Berlin, 2002), pp. 21–58.
[15] E. N. M. Cirillo and A. Muntean, Physica A (Amsterdam, Neth.) **392**, 3578 (2013).
[16] G. Albi, M. Bongini, E. Cristiani, and D. Kalise, SIAM J. Appl. Math. **76**, 1683 (2016).
[17] D. Helbing, I. Farkas, and T. Vicsek, Nature (London) **407**, 487 (2000).
[18] D. Helbing, L. Buzna, A. Johansson, and T. Werner, Transport. Sci. **39**, 1 (2005).
[19] R. Escobar and A. De La Rosa, in *Advances in Artificial Life, Proceedings of the 7th European Conference, ECAL, 2003, Dortmund, Germany, September 14–17, 2003*, Lecture Notes in Computer Science Vol. 2801, edited by W. Banzhaf, J. Ziegler, T. Christaller, P. Dittrich, and J. T. Kim (Springer, Berlin, 2003), pp. 97–106.
[20] A. Muntean, E. N. M. Cirillo, O. Krehel, and M. Bohm, in *Collective Dynamics from Bacteria to Crowds: An Excursion through Modeling, Analysis and Simulation*, edited by A. Muntean and F. Toschi (Springer, Berlin, 2014).
[21] E. N. M. Cirillo and A. Muntean, Comptes Rendus Mécanique **340**, 625 (2012).
[22] D. Braess, A. Nagurney, and T. Wakolbinger, Transport. Sci. **39**, 446 (2005).
[23] R. L. Hughes, Annu. Rev. Fluid Mech. **35**, 169 (2003).
[24] E. N. M. Cirillo, O. Krehel, A. Muntean, and R. van Santen, Phys. Rev. E **94**, 042115 (2016).
[25] E. N. M. Cirillo, O. Krehel, A. Muntean, R. van Santen, and S. Aditya, Physica A (Amsterdam, Neth.) **442**, 436 (2016).
[26] B. W. Fitzgerald, J. T. Padding, and R. van Santen, Phys. Rev. E **95**, 013307 (2017).
[27] A. Ciallella and E. N. M. Cirillo, Linear Boltzmann dynamics in a strip with large reflective obstacles: Stationary state and residence time, Kin. Relat. Models (to be published).
[28] W. Feller, *An Introduction to Probability Theory and Its Applications* (John Wiley & Sons, New York, 1968).
[29] E. N. M. Cirillo and M. Colangeli, Phys. Rev. E **96**, 052137 (2017).
[30] F. Stern, Math. Magazine **48**, 200 (1975).